

The Stark Anomalous Dispersion Optical Filter: The Theory

B. Yin and T. M. Shay

New Mexico State University, Las Cruces, New Mexico

The Stark anomalous dispersion optical filter is a wide-frequency-tunable ultra-narrow-bandwidth optical filter. The first theoretical investigation of this filter matched to the wavelength of a doubled Nd:YAG laser is reported. The calculations show that such a filter may provide above 80 percent transmission, and a noise equivalent bandwidth of 3 GHz.

I. Introduction

In a deep space laser communication system, a doubled Q-switched Nd:YAG laser is a potential laser transmitter. At the receiver end, in addition to a very weak signal with a large Doppler frequency shift (up to ± 77 GHz, typical for the Mars orbital missions), a considerable amount of background noise (sun, sunlit Earth, etc.) is expected within the field of view of the receiver. A high-sensitivity and high background-noise-rejection optical filter with wide-frequency tunability around the doubled Nd:YAG laser emission can simultaneously track Doppler frequency shifts and reject intense background radiation. The Stark anomalous dispersion optical filter (SADOF) is designed to provide high background noise rejection and wide frequency tunability and to operate at the wavelength of the doubled Nd lasers [1,2]. The SADOF is similar to our previously reported nontunable Faraday anomalous dispersion optical filter (FADOF) [3-5]. It may be considered as simply an addition of an electric field and optical pumping to the FADOF. In the following sections, the basic design and theoretical calculations are presented, the issues of shifting the SADOF center frequency using the Stark effect are investigated, and the calculation results for the SADOF operating at the doubled Nd:YAG laser line are discussed. These results have been used to direct the thrust of the experimental design.

II. Basic Design

Like the FADOF, the SADOF has a longitudinal magnetic field to induce the polarization rotation due to the resonant Faraday effect. However, in addition, the SADOF has an external electric field to shift the energy levels of the atoms. To use the resonant Faraday effect, an atomic transition that matches the Nd laser lines is required. To have a large energy level shift that results in a filter center frequency shift, a large scalar polarizability for an energy level in the filter transition is desired. Alkali atoms have large scalar polarizabilities, and the candidate transitions appropriate for doubled Nd laser lines are summarized in Table 1. For the transitions in Table 1, the lower states are the first or second excited states of the atoms, and the upper states are higher lying states. Since the lower-level state of the filter transition is not the ground state, optical pumping to populate the lower-level state is required

for filter operation at those transitions. The scalar polarizability is determined by examining the Stark Hamiltonian for the interaction between an atom and an electric field ε , which is

$$H_e = -\varepsilon(\mathbf{p}) \quad (1)$$

where \mathbf{p} is the induced dipole moment. For alkali elements, the perturbation of electrons in the closed shells may be neglected; then \mathbf{p} is given by

$$\mathbf{p} = -e\mathbf{r} \quad (2)$$

where \mathbf{r} is the position vector of the valence electron, and e is the electron charge. The high-lying states have much larger $\langle \mathbf{r} \rangle$, therefore, much stronger Stark interaction, or larger polarizabilities. Because the upper levels of the SADOE transitions in Table 1 are high-lying levels, their polarizabilities are large. For example, the scalar polarizability of the Rb(10S) state is about 280 MHz/(kV/cm)², while the scalar polarizability of the Rb(5P) state is only about 0.2 MHz/(kV/cm)².

Table 1. Potential SADOE lines in alkali vapors.

Transition	Wavelength (in air), nm	Compatible doubled Nd laser	Laser wavelength (air $T = 300$ K), nm
Rb 5P _{1/2} –8D _{3/2}	536.26	YALO	536.45
Rb 5P _{3/2} –9D _{5/2}	526.00	YLF	526.5
Rb 5P _{1/2} –10S _{1/2}	532.24	YAG	532.07 ^a
Rb 5P _{3/2} –10S _{1/2}	539.06	BEL	539.5
		YALO	539 ± 1
Rb 5P _{3/2} –11S _{1/2}	523.39	YLF	523.6
K 4P _{3/2} –6D _{5/2}	535.96	YALO	536.45
K 4P _{1/2} –8S _{1/2}	532.32	YAG	532.07 ^a
Cs 6P _{3/2} –13D _{5/2}	535.04	BEL	535.05

^aNd:YAG laser needs to be heated to about 100–150 deg C for the wavelength to match the filter.

Because the Rb 532-nm transition is the closest transition to the strongest line of doubled Nd:YAG laser, we discuss the Rb 532-nm SADOE Rb (5P_{1/2}–10S_{1/2}) in this article. The basic structure for an Rb 532-nm SADOE that operates at the doubled Nd:YAG laser line is shown in Fig. 1. An Rb vapor cell is placed between two crossed polarizers under the external longitudinal magnetic field and transverse electric field. The optical pumping is applied from one end of the cell. The colored-glass filter is used to ensure that the infrared pump radiation does not reach the photodetector.

III. The Energy Hamiltonian in the Presence of Magnetic and Electric Fields

When an electric field is applied to an atom, it shifts the electronic energy levels. This is known as the Stark effect, and the energy level shift is quadratically dependent on the electric field strength. The effective Hamiltonian element for the energy shift can be expressed as

$$\langle IJFM | H_e | IJF'M' \rangle = -\frac{1}{2}(\alpha_0 \delta_{FM, F'M'} + \alpha_2 Q_{FF', MM'}) \varepsilon^2 \quad (3)$$

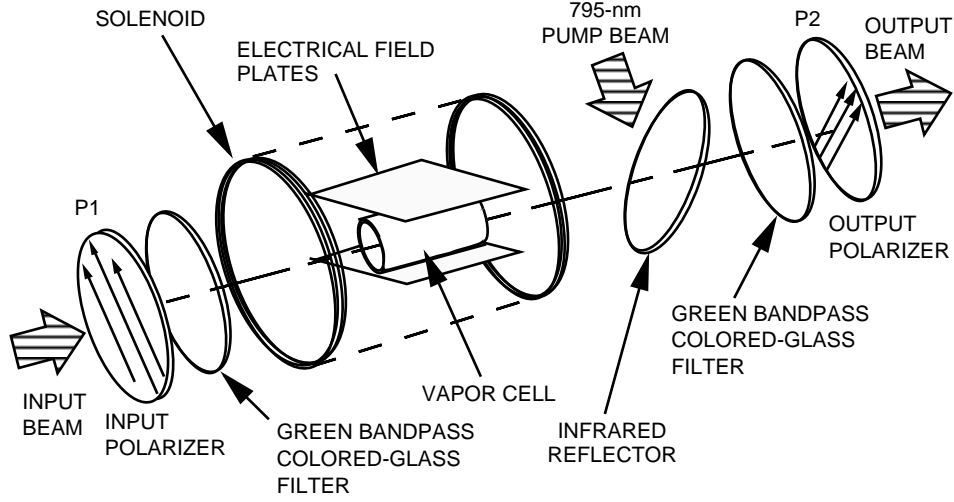


Fig. 1. The basic structure of an Rb 532-nm SADO.

where $J, I, F = J + I$, and M are the quantum numbers for the total orbital angular momentum, the nuclear spin, the total angular momentum, and the projection of total angular momentum, respectively. The values of α_0 and α_2 are the scalar and tensor polarizabilities, respectively. The delta function $\delta_{FM, F'M'}$ is unity only if $F = F'$ and $M = M'$; otherwise it is zero. The quadrupole matrix element between hyperfine states is $Q_{FF', MM'}$ [6], and its values are dependent on the quantum numbers of the sublevels. The $\delta_{FM, F'M'}$ weighting of α_0 in Eq. (3) shows that the change in energy level associated with the scalar polarizability term is common to all sublevels of a state, whereas the energy change associated with a tensor polarizability term differs for the various sublevels because of the $Q_{FF', MM'}$ factor. Because of the large scalar polarizability of the high-lying Rb $10S_{1/2}$ state, the energy level, i.e., frequency, of the optical transition can be shifted over a very large range using reasonable electric field strengths. The tensor polarizability is zero for all $J = 1/2$ states; hence, α_2 for the $10S_{1/2}$ and $5P_{1/2}$ states is zero.

Like the FADO theory, the theory for the transmission of the Rb 532-nm SADO begins by constructing the energy Hamiltonian. Assuming the Stark splitting is small compared with the fine structure, the element of the total energy Hamiltonian in the presence of an external electric field and magnetic field for the Rb 532-nm SADO is given by

$$\begin{aligned}
 \langle IJFM | H | IJF'M \rangle &= \{hyperfine\ energy\} + \{Stark\ energy\} + \{magnetic\ energy\} \\
 &= \Delta E_F \delta_{F, F'} - \frac{1}{2} \alpha_0 \varepsilon^2 \delta_{F, F'} + \left\{ \mu B_z (-1)^{M+J-1+I} g_J \right. \\
 &\quad \left. \times \sqrt{J(J+1)(2J+1)(2F+1)(2F'+1)} \begin{Bmatrix} J & 1 & J \\ F' & 1 & F \end{Bmatrix} \begin{pmatrix} F & 1 & F' \\ -M & 0 & M \end{pmatrix} \right\} \quad (4)
 \end{aligned}$$

where ΔE_F is the hyperfine energy shift caused by nuclear spin and is not influenced by external fields [5], μ is the Bohr magneton, B_z is the external magnetic field, and g_J is the Lande g factor that depends on J . The 6-j symbol (enclosed by the curly brackets) and the 3-j symbol (enclosed by the parentheses) are matrix representations of the spherical coordinate components of the electron wave function for the single atom. The hyperfine energy term and the magnetic energy term are exactly the same as in the FADO theory. Since the tensor polarizability is zero for $J = 1/2$, the only effect of the electric field in the Rb 532-nm SADO is to shift the center of gravity of an atomic energy level. Therefore, the atomic

transition intensities and polarization rotation calculations are the same as for the FADOF model, except that the atomic number density of the transition lower energy level will depend on the optical pumping. An energy level diagram depicting the Rb 532-nm SADOFF pumping is shown in Fig. 2.

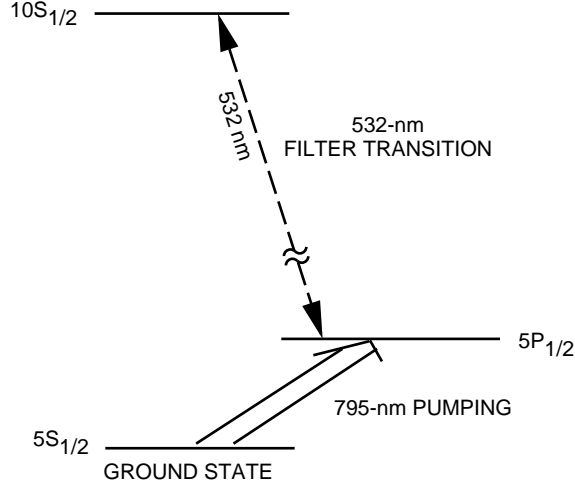


Fig. 2. A simplified Rb 532-nm SADOFF energy-level diagram.

Optical pumping is key to SADOFF operation. Significant transmission of the signal radiation is achieved only if the lower level atomic state $5P_{1/2}$ of the filter transition is sufficiently populated. We have developed a simple model to predict the required optical pumping. In this, our first SADOFF design, we have tailored the filter parameters to achieve operation at reasonable optical pumping powers and operating temperatures. Our analysis predicts that a 10-cm-long cell operating at a temperature of 190 deg C and pumped by 200 mW of optical power can demonstrate filter performance.

IV. SADOFF Transmission

To predict the SADOFF performance, the energy Hamiltonian, the hyperfine transition frequencies and line strengths, and the complex refractive indices need to be determined. The complex refractive indices are used to calculate the optical polarization rotation and absorption, and hence the filter transmission. This has been shown in our previous Rb FADOF articles [3–5]. The following is a brief summary of the equations necessary to predict the filter performance. The polarization rotation angles can be determined from complex refractive indices,

$$\phi(\omega) = \left(\frac{\omega L}{2c}\right) \text{Re}[\tilde{n}_+(\omega) - \tilde{n}_-(\omega)] \quad (5)$$

where \tilde{n}_{\pm} is the complex refractive index for the two circular polarizations, L is the cell length, and c is the speed of light. The absorption coefficient is given by

$$k_{\pm}(\omega) = \left(\frac{2\omega}{c}\right) \text{Im}[\tilde{n}_{\pm}(\omega)] \quad (6)$$

The transmission of the SADOFF filter is

$$T(\omega) = \frac{1}{4} \left\{ \exp[-k_+(\omega)L] + \exp[-k_-(\omega)L] - 2 \cos[2\phi(\omega)] \exp\left[-\frac{k_+(\omega) + k_-(\omega)}{2}L\right] \right\} \quad (7)$$

The equivalent noise bandwidth (ENBW) is expressed as

$$ENBW = \frac{1}{T_{max}} \int_0^{\infty} T(\omega) d\omega \quad (8)$$

where $T(\omega)$ represents the filter transmission spectrum, and T_{max} represents the maximum transmission for the filter. The equivalent noise bandwidth corresponds to the bandwidth of a rectangular notch filter with transmission T_{max} that transmits the same amount of noise as our filter. The equivalent noise bandwidth provides a ready comparison of different filter designs and even different kinds of optical filters.

V. Results and Discussion

A. Rotation and Transmission Spectrum

The SADOFF transmission spectrum was calculated using the equations presented in the previous sections. Figures 3 and 4 show the SADOFF rotation and transmission spectrum for a filter operating at a temperature of 190 deg C with 200 mW optical pumping, and in a magnetic field of 700 G.

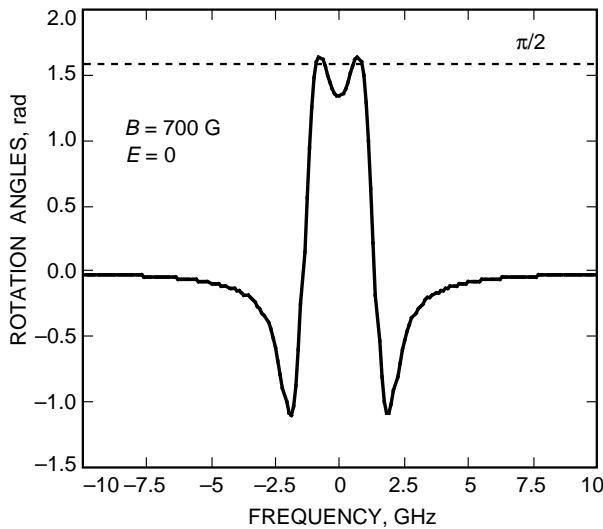


Fig. 3. Rb 532-nm SADOFF rotation angles versus frequency at $T = 190$ deg C and $B = 700$ G, where the horizontal axis is normalized to the frequency shift from the Rb 532-nm transition.

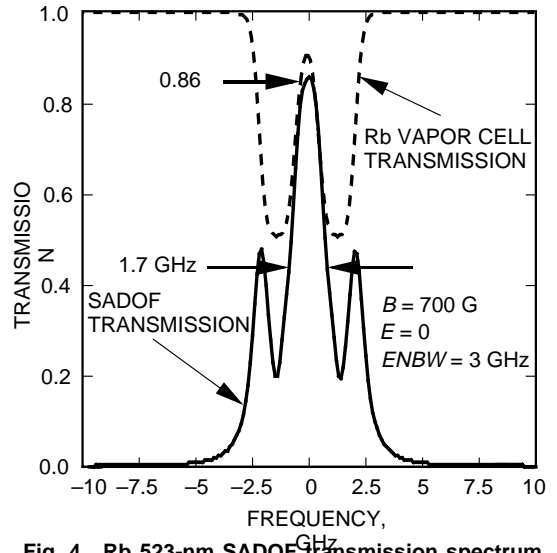


Fig. 4. Rb 523-nm SADOFF transmission spectrum at $T = 190$ deg C, $B = 700$ G, and $E = 0$ kV/cm, where the horizontal axis is normalized to the frequency shift from the 532-nm transition.

As in the FADOFF, the peak transmission occurs just outside the resonance absorption band where the rotation angle is nearly $-\pi/2$. Under these operating conditions, the SADOFF has a peak transmission of about 0.86, a 1.7-GHz bandwidth across the principal transmission peak, and equivalent noise bandwidth of 3.0 GHz.

The SADOFF center frequency is tuned by varying the electric field. Figure 5 shows the predicted E-field frequency shift of the SADOFF transmission spectrum. The filter is in a 20-kV electric field, and the transmission spectrum is red-shifted about 55 GHz without any degradation in filter performance.

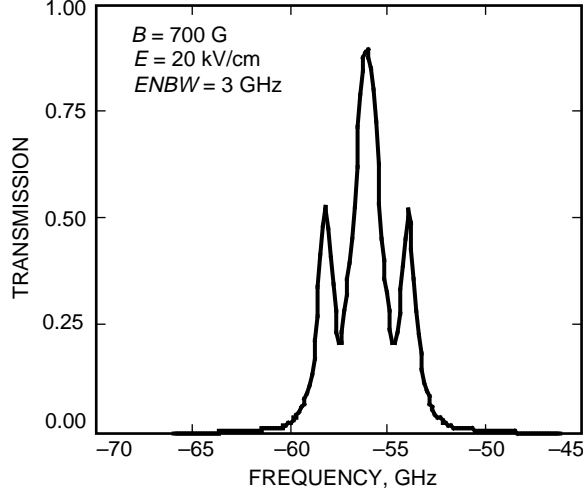


Fig. 5. Rb 532-nm SADOE transmission spectrum at $T = 190$ deg C, $B = 700$ G, and $E = 20$ kV/cm.

B. Frequency Tunability

Because the scalar polarizability in the upper energy level is much larger than the scalar polarizability in the lower level, the upper energy-level shifts determine to a good approximation the Rb 532-nm transition center frequency shift. Therefore, the filter center frequency shift depends quadratically on the electric field,

$$\Delta\nu = -\frac{1}{2}\alpha_0(10S_{1/2})\varepsilon^2 - \left[-\frac{1}{2}\alpha_0(5P_{1/2})\varepsilon^2 \right] \approx -\frac{1}{2}\alpha_0(10S_{1/2})\varepsilon^2 \quad (9)$$

The calculated center frequency shift of the filter passband versus the electric field is plotted in Fig. 6. It shows that the center frequency is shifted by about 250 GHz, or 0.25 nm by a 40-kV/cm field.

C. Optimized Operating Conditions

Figure 7 gives a series of transmission curves with different operating conditions. These curves are for different B-fields and temperatures and can be used to tailor the SADOE performance to the specific application based on the ENBW and peak transmission requirements.

This figure is calculated for a zero electric field since adding the electric field only tunes the center frequency. These curves also demonstrate that the bandwidth of the transmission can be varied by changing the magnetic field and the temperature.

D. Noise Leakage From Adjacent Filter Lines

The nearest green transition for the Rb 532-nm SADOE is the Rb ($5P_{1/2}-8D_{3/2}$) 536.3-nm transition. This transition can contribute a background noise component to the Rb SADOE. However, radiation from this and other Rb green transitions can be suppressed by using a commercial interference filter ($BW \approx 6$ nm) as a prefilter. The transition probability of Rb $5P_{1/2}-8D_{3/2}$ is seven times larger than the Rb $5P_{1/2}-10S_{1/2}$; the equivalent noise bandwidth of the $5P_{1/2}-8D_{3/2}$ transition is much larger than that of the $5P_{1/2}-10S_{1/2}$. The calculated ENBW for the Rb $5P_{1/2}-8D_{3/2}$ transition at a temperature of 190 deg C and a magnetic field of 700 G is 8 GHz. A lower ENBW (~ 3 GHz) can be achieved by using a narrower bandpass prefilter.

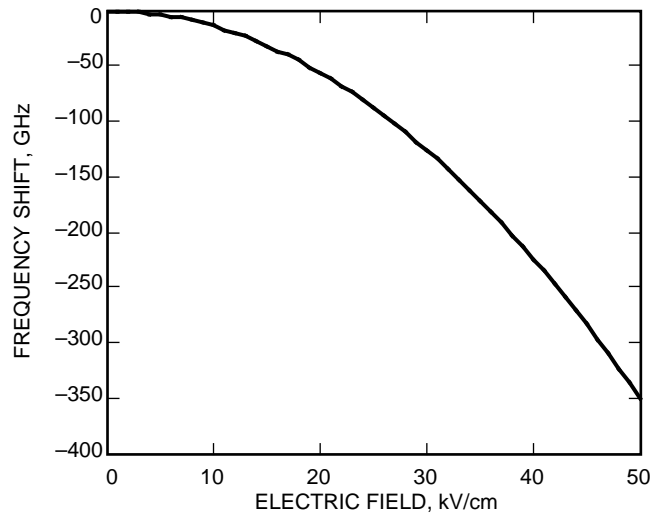


Fig. 6. Rb 532-nm SADO center frequency versus external electric field.

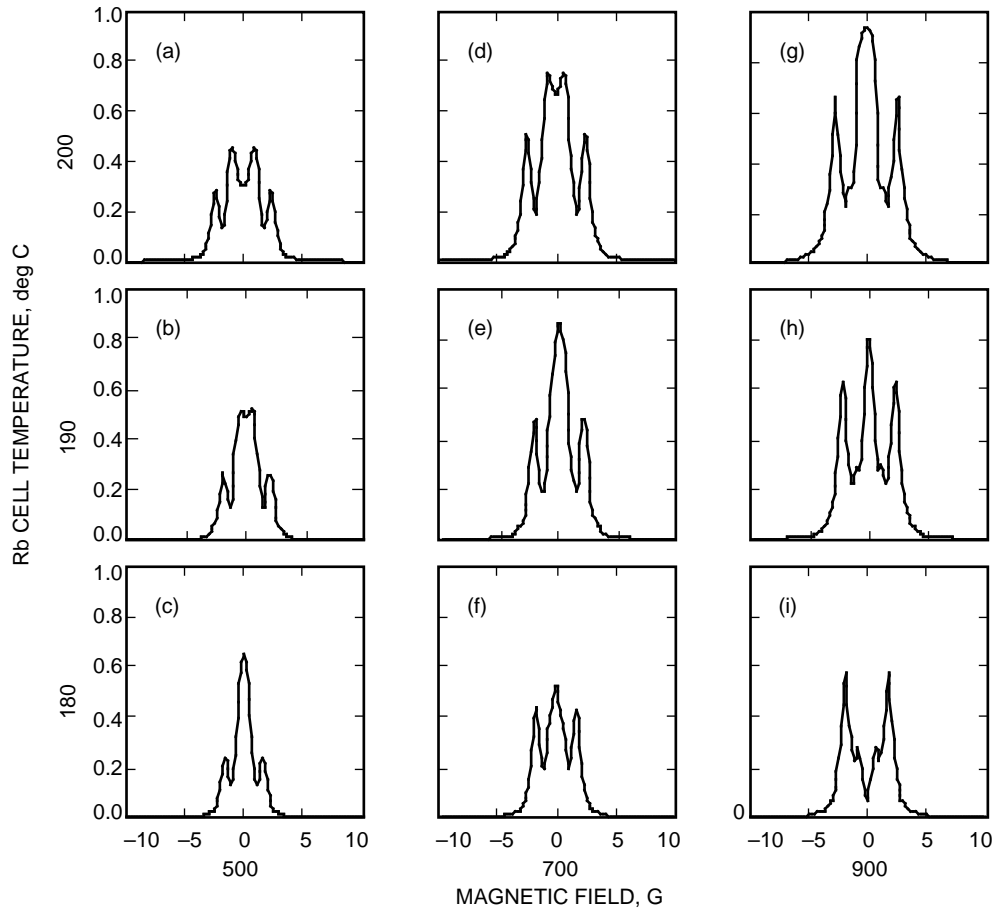


Fig. 7. Rb 532-nm SADO transmission spectrum at $E = 0$ and at (a) 500 G, 200 deg C, $ENBW = 3.9$ GHz; (b) 500 G, 190 deg C, $ENBW = 3.2$ GHz; (c) 500 G, 180 deg C, $ENBW = 2.0$ GHz; (d) 700 G, 200 deg C, $ENBW = 4.2$ GHz; (e) 700 G, 190 deg C, $ENBW = 3.0$ GHz; (f) 700 G, 180 deg C, $ENBW = 3.2$ GHz; (g) 900 G, 200 deg C, $ENBW = 4.0$ GHz; (h) 900 G, 190 deg C, $ENBW = 3.4$ GHz; and (i) 900 G, 180 deg C, $ENBW = 3.0$ GHz.

VI. Conclusions

The first theoretical model for calculating the performance of the SADOFF is developed. The operating conditions for a 532-nm SADOFF are determined. The filter is compatible with the strongest line of a frequency-doubled Nd:YAG laser. The results show that the SADOFF can provide very narrow bandwidth, high transmission, low equivalent noise bandwidth, and, most of all, can be tuned over a very large frequency range (250 GHz at $E = 40$ kV/cm). The SADOFF is a good candidate for a filter in the deep space laser communications using a doubled Nd:YAG laser as a source.

Acknowledgments

The authors wish to thank Drs. K. Wilson and J. R. Lesh in the JPL Optical Communications Group for reviewing this work.

References

- [1] B. Yin and T. M. Shay, "Theoretical Model for a Stark Anomalous Dispersion Optical Filter," *Proc. Laser '92*, Houston, Texas, pp. 837–843, December 1992.
- [2] B. Yin and T. M. Shay, "A Rb 532 nm Stark Anomalous Dispersion Optical Filter for Doubled Nd:YAG Lasers," *Proc. LEOS '93*, San Jose, California, pp. 359–360, November 1993.
- [3] D. J. Dick and T. M. Shay, "Ultra-High Noise Rejection Optical Filter," *Opt. Lett.*, vol. 16, p. 867, June 1991.
- [4] B. Yin and T. M. Shay, "Theoretical Model of Faraday Anomalous Dispersion Optical Filter," *Opt. Lett.*, vol. 16, pp. 1617–1619, October 1991.
- [5] B. Yin, L. S. Alvarez, and T. M. Shay, "The Rb 780-Nanometer Faraday Anomalous Dispersion Optical Filter: Theory and Experiment," *The Telecommunications and Data Acquisition Progress Report 42-116*, vol. October–December 1993, Jet Propulsion Laboratory, Pasadena, California, pp. 71–85, February 15, 1994.
- [6] H. L. Zhou and B. W. Norcross, "Improved Calculation of the Quadratic Stark Effect in the $6P_{3/2}$ State of Cs," *Phys. Rev. A*, vol. 40, no. 9, pp. 5048–5051, November 1989.